Ion-Dependent Mobility Effects of the *Fusobacterium nucleatum* Glycine Riboswitch Aptamer II *Via* Site-Directed Spin Labeling (SDSL) Electron Paramagnetic Resonance (EPR)

Michelle A. Ehrenberger[a], Aleida Vieyra[a], Jackie M. Esquiaqui[a], Gail E. Fanucci[a,*]

[a]Department of Chemistry, University of Florida, P.O. Box 117200, Gainesville, FL 32611, United States

*Corresponding author: gefanucci@gmail.com

Abstract

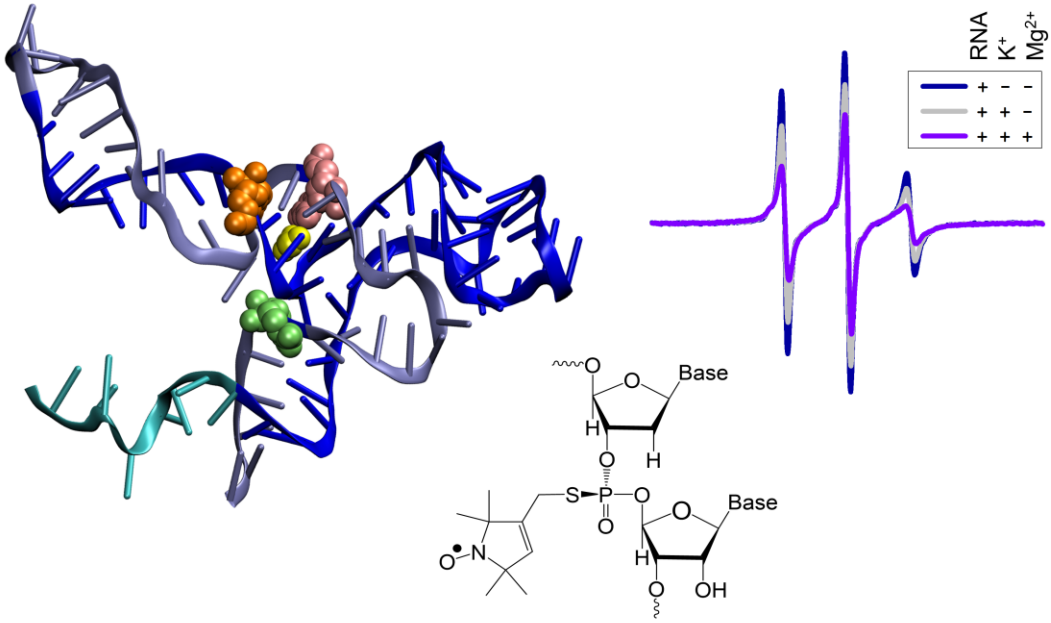

Site-directed spin labeling (SDSL) with continuous wave electron paramagnetic resonance (cw-EPR) spectroscopy was utilized to probe site-specific changes in backbone dynamics that accompany folding of the isolated 82 nucleotide aptamer II domain of the *Fusobacterium nucleatum* (*FN*) glycine riboswitch. Spin-labels were incorporated using splinted ligation strategies. Results show differential dynamics for spin-labels incorporated into the backbone at a basepaired and loop region. Additionally, the addition of a biologically relevant concentration of 5 mM Mg^{2+}, to an RNA solution with 100 mM K^{+}, folds and compacts the structure, inferred by a reduction in spin-label mobility. Additionally, when controlling for ionic strength, Mg^{2+} added to the RNA induces more folding/less flexibility at the two sites than RNA with K^{+} alone. Addition of glycine does not alter the dynamics of this singlet aptamer II, indicating that the full length riboswitch construct may be needed for glycine binding and induced conformational changes. This work adds to our growing understanding of how splinted-ligation SDSL can be

utilized to interrogate differential dynamics in large dynamic RNAs providing insights into how RNA folding and structure is differentially stabilized by monovalent versus divalent cations.

Keywords

site-directed spin-labeling (SDSL), electron paramagnetic resonance (EPR), riboswitch, splinted ligation, RNA, glycine

1. Introduction

Riboswitches are functional, non-coding RNA elements that bind a ligand usually related to the downstream genes they regulate. A riboswitch consists of a ligand-binding aptamer and a downstream effector called the expression platform domain (EPD). The riboswitch aptamer undergoes a conformational change upon ligand binding that modulates the structure of the EPD to affect gene expression. The glycine riboswitch is notable in that it consists of two aptamer domains, where each binds one molecule of glycine, linked to a single EPD. It was previously thought that the tandem aptamers functioned cooperatively, but this cooperativity was abolished by the inclusion of a leader sequence upstream of aptamer I that forms a highly conserved duplex with the linker sequence between aptamer I and aptamer II [1]. It is now believed that glycine binding enhances, and is enhanced by, interaptamer interactions upon ligand binding [2]. Fundamental questions still remain, however, regarding the dynamics of the riboswitch as it folds in the presence or absence of ligand as well as the necessary counterions [3]. Answers to these questions can be obtained from SDSL EPR investigations.

This study uses X-band continuous wave electron paramagnetic resonance (cw-EPR) with nitroxide spin-labels incorporated into the phosphate backbone such that differences in mobility can be observed upon folding with monovalent K^+ versus divalent Mg^{2+} ions and ligand (glycine) in solution. X-band cw-EPR is a useful tool for probing dynamics at a specific site in the RNA molecule when site-directed spin-labeling (SDSL) is employed [4]. In this method, an RNA construct is synthesized with a modification that allows for the chemical attachment of a moiety containing an unpaired electron that can be probed with EPR. Line shape analysis of the cw-EPR spectrum provides information about the spin-labeled site's relative mobility—which

includes both the rate of motion (dynamics) and the relative disorder or flexibility (order) [5-7]—and can be used as a measure of relative folding and compaction of the RNA. Because of synthetic limits to RNA length, we utilize splinted ligation techniques to covalently join shorter RNAs to form a larger RNA construct [8]; alternative methods for spin-labeling large RNAs are also emerging in the field [9-14].

Here, SDSL EPR is used to differentiate dynamics in aptamer II (84 nucleotides) of the *Fusobacterium nucleatum (FN)* glycine riboswitch [15,16] (Fig. 1A-D). Two spin labeled sites were chosen that were expected to reveal differential backbone dynamics upon folding due to structure: one in a base-paired region near the glycine binding site (A115), and one in a loop region further downstream (A153). The impact of a glycine binding mutation (U141A) [2] on dynamics was also investigated. Splinted ligation of two smaller synthetic fragments was used to generate each spin-labeled construct.

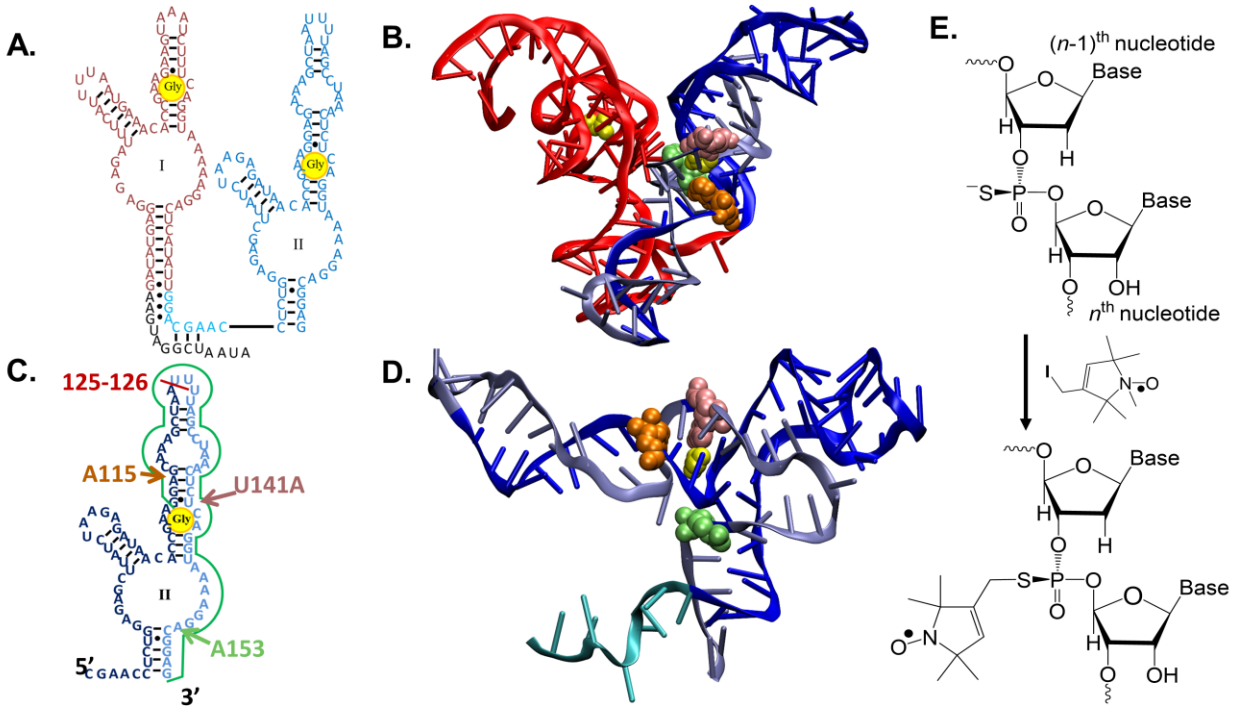

Fig. 1. Aptamers and crystal structure for the *FN* glycine riboswitch, along with the SDSL scheme. Secondary and tertiary structure (PDB 3P49) of the tandem aptamer (A & B) and aptamer II (C & D) with glycine in yellow; (B-D) show the glycine binding mutation in pink, A115 in orange, and A153 in green. In (C), the splinted ligation site is indicated by a red line (between nucleotides 125 and 126), and the DNA splint complementary region is indicated by a green line. (E) Phosphorothioate backbone labeling scheme with the R5 nitroxide spin label [17].

2. Materials and Methods

2.1. Synthetic RNA preparation and spin labeling

Synthetic RNA oligomers (Table S1) were purchased from Dharmacon (Pittsburgh, PA) with a deoxynucleotide (to prevent autohydrolysis) prior to a phosphorothioate modification, and processed as previously described [15]. Phosphorothioate modifications were modified with an R5 nitroxide made from an R5 precursor (Toronto Research Chemicals, Inc., Toronto, Ontario) using a previously published protocol [18,19] before splinted ligation (Fig. 1E).

2.2. RNA splinted ligation and purification

For each *FN* glycine riboswitch aptamer II, a 51 nt RNA was ligated to a 33 nt RNA *via* a protocol from a published method [20]. To anneal the DNA splint (IDT, Coralville, IA, Table S1provides all sequences of RNA fragments and DNA splint), 1 nmole of each RNA fragment (51 nt and 33 nt) were combined with 0.9 nmole of the DNA splint in 0.5 M NaCl. Each reaction was heated to 95°C, annealed, and ligated as described, previously [2,19], with the following modifications. Annealing was performed to equilibration at around 10°C in a 4°C incubator. After ligation, reactions were concentrated using a speed vac system (Centrivap concentrator and cold trap from Labconco, Kansas City, MO, with Model 2025 Dry Vacuum by Welch, Mt. Prospect, IL). Phenol Chloroform Isoamyl alcohol (PCA) extraction and ethanol precipitation

were performed before isolating the ligated product by gel purification on 10% or 20% denaturing PAGE gels. After the RNA was visualized by UV shadowing with a transiluminator and TLC plate, the 84 nt product bands were excised and eluted with mixing by rotation over 24-72 hours at room temperature in 600 μL TE buffer containing 10mM Tris-HCl and 1mM EDTA pH 8.0. The eluted RNA was extracted again with PCA and precipitated with ethanol. The recovered RNA was dissolved in autoclaved, nanopure water, and the concentration was determined by UV-vis spectroscopy (Cary 50 Bio from Varian, Palo Alto, CA).

2.3. EPR data collection and analysis

Along with RNA-only control samples (RNA in nanopore 18 MΩ water that may contain residual ions such as Na^+ or Cl^- from preparation procedures but no K^+ or Mg^{2+}), samples were prepared with biologically relevant concentrations of 100 mM K^+, 5 mM Mg^{2+}, and 5 mM glycine (Fig. 2C) [8] with reagents from Fisher Scientific (Pittsburgh, PA). To control for ionic strength, solutions were made with 15 mM, 100 mM, or 115 mM ionic strength KCl, $MgCl_2$, or a 86.96 : 13.04 ratio of KCl : $MgCl_2$ (Fig. 2D, 86.96 : 13.04 is the same ratio as a combination of biologically relevant concentrations, above). Ionic strengths were calculated with the equation $I = \frac{1}{2}\sum c_i {z_i}^2$ where I is the ionic strength of the solution, z_i is the charge on each ion, and c_i is the concentration of each ion [21]. To determine the effect of glycine on each ionic condition, solutions were made with or without glycine (Fig. 3B). EPR samples, each 3 μL, had an average spin concentration of 96 ± 10 μM and RNA concentration of 100 ± 20 μM determined by absorbance at 260nm. Spin concentration was determined by measuring the double integrated area of a non-normalized EPR spectrum, which was converted to concentration *via* standard

curve. Each sample was loaded into a 0.60 mm inner diameter, 0.84 mm outer diameter glass capillary tube (Fiber Optic Center, New Bedford, MA), flame-sealed at one end [8].

Spectra (Fig. S1) were recorded at X-band (9.5 GHz) cw-EPR on a Bruker E500 spectrometer with a loop gap resonator from Medical Advances (Milwaukee, WI). Measurements were taken with 23 dB power attenuation, 0.8 G modulation amplitude, 100 kHz modulation frequency, 100 G scan, averaging 10 scans. Temperature was stabilized at 25 ± 0.2°C as previously published [15].

Labview based software was used to baseline correct and determine $h_{(+1)}$ and $h_{(0)}$ intensities. Triplicate spectra were acquired for all constructs in each experimental condition, and $h_{(+1)}/h_{(0)}$ *values* are reported as average values from triplicate spectra and from replicated samples where possible (Table S2), with the greatest standard deviation found from sample replicate $h_{(+1)}/ h_{(0)}$ values of a single construct —a value of 0.02 for A153-labeled wild-type in 100mM K^+ and 5mM Mg^{2+} (Fig. S2)—was applied as the error to all measurements in the study, as a conservative error due to sample preparation. Student's t-test was used to determine significance.

2.4. In-line probing

Dephosphorylation, ^{32}P end-labeling, in-line probing, T1 digestion, alkaline digestion, and dPAGE analysis were carried out as described in Regulski and Breaker [22], except that the in-line reaction buffer was made without Mg^{2+}, and the RNA was heated at 95°C for 3 minutes and cooled to 21°C before adding Mg^{2+} to a final concentration of 20 mM and letting stand at room

temperature between 40 and 48 hours. Results were visualized using an Amersham Typhoon imager from GE Healthcare (Pittsburgh, PA) and ImageQuant 7.0 (GE Healthcare).

3. Results

EPR spectra and analysis that characterize the local folding and dynamics of the four *FN* glycine riboswitch aptamer II constructs are shown in Fig. 2. Because motion averages the effects of the hyperfine anisotropy of the nitroxide spectra [5-7,23], the mobility of the spin label can be characterized by empirical line shape parameters. For this work, the ratio of the intensities of the low field and central field transitions ($h_{(+1)}/ h_{(0)}$) [15], was chosen as a means to quantitatively compare the mobility of the R5 nitroxide at the backbone labeled A153 and A115 sites (Fig. 2A&B). Parameter values close to 1 reflect nearly isotropic motion with sub-nanosecond correlation times; whereas values that decrease to ~ 0.3 reflect slowed motion, but still faster than a correlation time of 1 ns that may have some degree of anisotropy [24].

Results for $h_{(+1)}/ h_{(0}$ analysis of EPR spectra are shown in Fig. 2 C&D (All spectra are given in Supporting Information, Figure S1). RNA folding is greatly stabilized and often requires cations due in part to the polyanionic nature of the RNA backbone [3]. Even in the absence of added ions and ligand, A115-R5 experiences restricted mobility, $h_{(+1)}/ h_{(0)}$=0.54 (Fig. 1B&C) compared to A153-R5, $h_{(+1)}/ h_{(0)}$=0.78 (Fig. 1A&C; for comparison, $h_{(+1)}/ h_{(0)}$=0.89 was obtained for a labeled 20 nt synthetic RNA fragment [25]), indicating that the A115-containing portion of the RNA may be partially folded even in the absence of added K^+ or Mg^{2+}, perhaps due to residual Na^+ from sample preparation. Additionally, in each of the environmental conditions tested, the spin-label backbone at A115-R5 shows reduced mobility compared to A153-R5 ($p<0.01$). This

result is expected, as A115 is located within a base-paired stem region of the aptamer, whereas A153 is located in a loop region that would likely be more flexible. These results add to the body of evidence that differential dynamics within regions of an RNA macromolecule can be characterized by cw-EPR [4,5,8,9,15,23], due to differences in flexibility within a single strand.

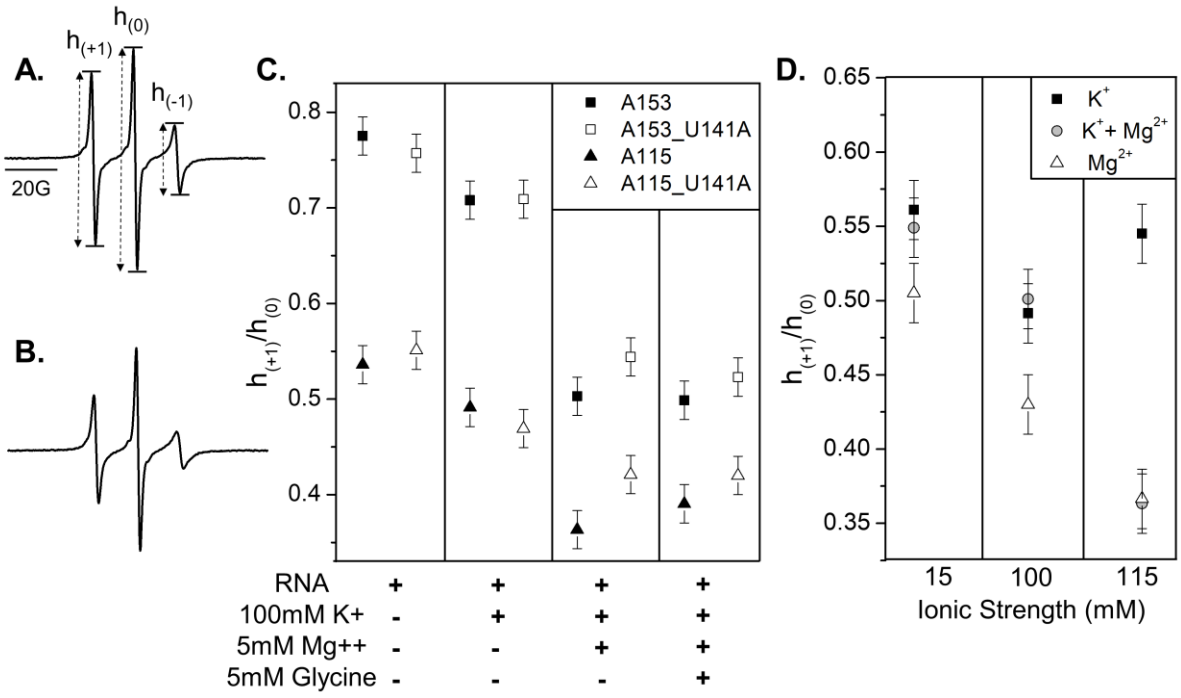

Fig. 2. Example spectra as well as $h_{(+1)}/h_{(0)}$ analysis for A153- and A115-labeled sites, with and without glycine binding mutant (U141A) under varied solution conditions. Example 100 G X-band CW-EPR spectra for RNA-only (A) A153-R5 and (B) A115-R5. (C) Plot of mobility parameter ($h_{(+1)}/h_{(0)}$) for A115-R5 and A153-R5 wild-type and binding mutant in biologically relevant solution conditions. (D) Plot of mobility parameter for A115-R5 iso-ionic strength solutions with one ion or two ion species.

For both spin labeled sites, only a slight decrease in mobility is observed upon addition of K^+ ($p<0.05$ at A115-R5, $p<0.02$ at A153-R5) with more enhanced decrease upon addition of Mg^{2+}

($p<0.01$), and essentially no change upon further addition of glycine. This result contrasts our earlier findings where addition of K^+ fully induced the folding of the *VC* glycine riboswitch leader-linker sequence [8]. Thus, the current work involving *FN* aptamer II shows a novel finding, because both A153 and A115 sites show a Mg^{2+} dependent folding inferred from changes in backbone spin-label mobility.

Incorporation of the U141A glycine binding mutation in the presence of K^+ with Mg^{2+} ($p<0.05$) induces a slightly greater mobility than in the wild-type for A115-R5, where mobility changes forA153-R5 were not statistically different within errors. This impact of U141A may be understood by considering the close proximity between nucleotides 141 and A115-R5 in the secondary helix structure of the aptamer, where the mutation may slightly disrupt the helix, preventing the level of compaction seen in the wild-type. Interestingly, glycine addition does not alter the mobility of *any* of the four constructs, within error (discussed more below).

A natural question arises as to the impact of ion identity versus ionic strength on inducing the fold observed in aptamer II. The EPR data in Fig. 2C reflect solution conditions with biologically relevant concentrations of K^+ and Mg^{2+}. Fig. 2D summarizes A115-R5 mobility as ionic strength is altered (15 mM, 100 mM, and 115 mM) for K^+, Mg^{2+}, and both ions. At each ionic strength, lower mobility is observed with Mg^{2+} than iso-ionic strength K^+ ($p<0.05$ at 15 mM, $p<0.02$ at 100 mM, $p<0.01$ at 115 mM), indicating that ion identity is important for the compaction of the RNA at the tested site.

The effect of the K^+ plus Mg^{2+} combination is similar to that of K^+ alone at both 15 mM and 100 mM ionic strengths, but more closely mimics that of Mg^{2+} at 115 mM ionic strength. In this 115 mM combination, Mg^{2+} contributes only an ionic strength of 15 mM (13.04% of 115 mM, *see Materials and Methods*), showing that a small amount of Mg^{2+} appears to act synergistically with higher concentrations of K^+. Results indicate that both ionic strength and ion identity can impact the folding/compaction of this aptamer.

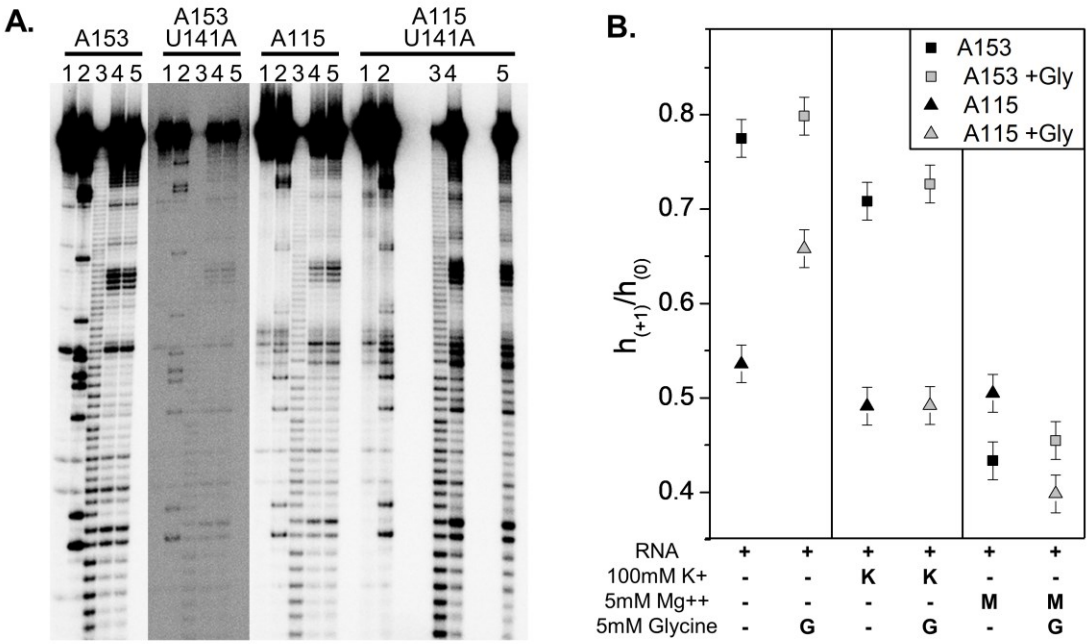

Fig. 3. Glycine may not bind aptamer II singlet. (A) In-line probing results verify a lack of structural change upon glycine addition to a solution including K^+ and Mg^{2+}. (1) Uncleaved RNA, (2) T1 digested RNA cut 5′ to each G residue, (3) Alkaline digest cleaving each nucleotide, (4) inline probing in the presence of K^+ and Mg^{2+} without glycine, (5) inline probing with K^+, Mg^{2+}, and 1mM glycine. Data for A153_U141A samples are shown at higher contrast due to lower labeling efficiency of the sample. (B) Plot of mobility parameter comparing solution conditions with and without glycine for RNA only (*see Materials and Methods)*, RNA with K^+, and RNA with Mg^{2}+.

Although glycine addition did not modulate spin-label mobility at either A153-R5 or A115-R5 in the presence of both ions (Fig. 2C) or alter secondary structure as seen by inline probing with both ions (Fig. 3A), we considered the hypothesis that perhaps glycine addition might alter RNA backbone dynamics/folding when only one ion species, or neither, was present. Therefore, EPR measurements were collected for both spin-labeled sites under various conditions (Fig. 3A). Most conditions investigated yielded little to no change in backbone mobility with the addition of glycine. However, under two conditions we studied, alterations in backbone dynamics resulted from addition of glycine. Strangely, an *increase* in mobility ($p<0.01$) was observed in the RNA only condition at A115-R5, which is located in a base-paired helix. This finding may reflect that glycine is acting as an osmolyte and decreasing the stability of the RNA secondary structure in the absence of Mg^{2+} since nucleotide bases preferentially interact with some amino acids over water, shifting equilibrium toward the unfolded state [26]. Again, we note that the mobility observed in Fig. 2C for A115-R5 in water alone is lower ($h_{(+1)}/ h_{(0)}$=0.53; τ_{corr} ~ 0.8 ns) [15] than expected for an unfolded RNA, so this aptamer may misfold in water (or fold due to residual Na^{+} from sample preparation) and glycine addition may cause an unfolding.

In contrast, a slight *decrease* in local motion was also observed at A115-R5 when 5 mM glycine was added to the RNA already in 5 mM Mg^{2+} ($p<0.01$). We are surprised by this observation because a recent report showed that a single glycine riboswitch aptamer, or "singlet" can bind glycine only when a portion of the other aptamer containing vital interaptamer contacts—a "ghost" aptamer—is also present [27]; which would imply that our aptamer II should not bind glycine. Although further experiments would be needed to unequivocally determine whether our aptamer II construct binds its native ligand, we chose not to pursue this further as our on-going

future work targets the full-length *FN* glycine riboswitch where the biologically relevant RNA will be investigated. Despite the apparent lack of glycine binding induced structural changes in folding or mobility, the current work reveals the novel finding that some features in the glycine riboswitch, such as the linker-leader interaction, are fully folded by K^+ while others require Mg^{2+} to reach their fully folded state.

4. Discussion

SDSL EPR offers methodology to interrogate in a site-wise manner how solution conditions impact the mobility of dynamic RNAs by inducing folded states [5,7,25]. Previously, we found that 100 mM K^+-induced folding of the kink-turn motif of the *VC* glycine riboswitch without further reduction in mobility upon addition of Mg^{2+} and glycine [8,15]. Here, we find that 100 mM K^+ alone is not sufficient to fully fold aptamer II of the *FN* glycine riboswitch, and Mg^{2+} is required to reach the fully compacted state. This ability of divalent Mg^{2+} to fold aptamer II to a greater extent than monovalent K^+ has been demonstrated at three different ionic strengths of solution, and is consistent with prior thermodynamic analysis of the effects of K^+ and Mg^{2+} on RNA folding, particularly secondary and tertiary folding, respectively [3]. Other recent EPR investigations on the tetracycline-binding RNA aptamer also demonstrate Mg^{2+} modulation of the fold and compaction [28].

No change in mobility was observed for *FN* aptamer II constructs when glycine was added to a solution with biologically relevant concentrations of K^+ and Mg^{2+}, likely indicating that the singlet aptamer either does not bind glycine or exists in a pre-formed state ready to bind glycine, although we suspect the former. Additionally, aptamer II of the *VC* riboswitch has been shown

to homodimerize at lower concentrations than those tested here [2] in the presence of K^+ and Mg^{2+}, as well as both ions and glycine. DEER dipolar oscillation curves showed no evidence of dimerization (data not shown), indicating that our construct in solution may be monomeric. Further experiments, such as native gel-shift assays or HPLC, could be used to determine the oligomerization of this aptamer II construct, but instead we will prioritize experiments on the full-length riboswitch in future.

Our future efforts focus on utilizing this SDSL approach to characterize changes in backbone dynamics at select sites in various structural elements in the full-length *FN* glycine riboswitch to address how aptamer fold is impacted by ions, ionic strength, glycine binding, and interaptamer interactions. Future work will also include a functional model of an EPD. Prior work of others predicts that within the full riboswitch, aptamer II folding may depend on interaction with the EPD sequence [2]. The researchers proposed that the glycine riboswitch exists in equilibrium between an unfolded and a folded, glycine-bound state. In the unfolded state, the EPD is sequestered from performing its regulatory function by forming a base-paired helix with a portion of aptamer II. In the folded state, however, the two aptamers each bind a ligand and fold together using interaptamer contacts, leaving the EPD free to affect gene expression [2]. This model for *FN* follows the demonstrated folding states in *Bacillus subtilis* by Mandal et al [29].

The cw-EPR results clearly demonstrates that SDSL EPR can differentiate between the local motion at different sites within large dynamic RNA molecules where local conformation can be modulated by both the identity and ionic strength of the ions in solution. Our combined SDSL

studies on glycine riboswitch domains show that different regions of this dynamic RNA require different ionic environments to be stabilized in their folded states.

Acknowledgements

The authors thank Dr. Michael E. Harris and Dr. Jing Zhao for their materials and expertise in assisting with the in-line probing experiments. This work was supported by the National Science Foundation [grant number MCB-1715384 (G.E.F.) and DGE-0802270 (J.M.E.)], and instrumentation was supported by the National Institute of Health [grant number S10RR031603].

References

[1] E.M. Sherman, J. Esquiaqui, G. Elsayed, J.D. Ye, An energetically beneficial leader-linker interaction abolishes ligand-binding cooperativity in glycine riboswitches, Rna-a Publication of the Rna Society 18 (2012) 496-507. 10.1261/rna.031286.111.
[2] K.M. Ruff, S.A. Strobel, Ligand binding by the tandem glycine riboswitch depends on aptamer dimerization but not double ligand occupancy, Rna-a Publication of the Rna Society 20 (2014) 1775-1788. 10.1261/rna.047266.114.
[3] D. Leipply, D. Lambert, D.E. Draper, ION-RNA INTERACTIONS: THERMODYNAMIC ANALYSIS OF THE EFFECTS OF MONO- AND DIVALENT IONS ON RNA CONFORMATIONAL EQUILIBRIA, Methods in Enzymology, Vol 469: Biophysical, Chemical, and Functional Probes of Rna Structure, Interactions and Folding, Pt B 469 (2009) 433-463. 10.1016/s0076-6879(09)69021-2.
[4] P.Z. Qin, J. Iseri, A. Oki, A model system for investigating lineshape/structure correlations in RNA site-directed spin labeling, Biochem Biophys Res Commun 343 (2006) 117-124. 10.1016/j.bbrc.2006.02.138.
[5] P. Nguyen, P.Z. Qin, RNA dynamics: perspectives from spin labels, Wiley Interdisciplinary Reviews-Rna 3 (2012) 62-72. 10.1002/wrna.104.
[6] W.L. Hubbell, C.J. Lopez, C. Altenbach, Z.Y. Yang, Technological advances in site-directed spin labeling of proteins, Current Opinion in Structural Biology 23 (2013) 725-733. 10.1016/j.sbi.2013.06.008.
[7] G.E. Fanucci, D.S. Cafiso, Recent advances and applications of site-directed spin labeling, Current Opinion in Structural Biology 16 (2006) 644-653. 10.1016/j.sbi.2006.08.008.
[8] J.M. Esquiaqui, E.M. Sherman, S.A. Ionescu, J.D. Ye, G.E. Fanucci, Characterizing the Dynamics of the Leader-Linker Interaction in the Glycine Riboswitch with Site-Directed Spin Labeling, Biochemistry 53 (2014) 3526-3528. 10.1021/bi500404b.
[9] E.S. Babaylova, A.A. Malygin, A.A. Lomzov, D.V. Pyshnyi, M. Yulikov, G. Jeschke, O.A. Krumkacheva, M.V. Fedin, G.G. Karpova, E.G. Bagryanskaya, Complementary-addressed site-

directed spin labeling of long natural RNAs, Nucleic Acids Research 44 (2016) 7935-7943. 10.1093/nar/gkw516.
[10] L. Buttner, F. Javadi-Zarnaghi, C. Hobartner, Site-Specific Labeling of RNA at Internal Ribose Hydroxyl Groups: Terbium-Assisted Deoxyribozymes at Work, Journal of the American Chemical Society 136 (2014) 8131-8137. 10.1021/ja503864v.
[11] M. Kerzhner, D. Abdullin, J. Wiecek, H. Matsuoka, G. Hagelueken, O. Schiemann, M. Famulok, Post-synthetic Spin-Labeling of RNA through Click Chemistry for PELDOR Measurements, Chemistry-a European Journal 22 (2016) 12113-12121. 10.1002/chem.201601897.
[12] M. Kerzhner, H. Matsuoka, C. Wuebben, M. Famulok, O. Schiemann, High-Yield Spin Labeling of Long RNAs for Electron Paramagnetic Resonance Spectroscopy, Biochemistry 57 (2018) 2923-2931. 10.1021/acs.biochem.8b00040.
[13] S. Saha, T. Hetzke, T.F. Prisner, S.T. Sigurdsson, Noncovalent spin-labeling of RNA: the aptamer approach, Chemical Communications 54 (2018) 11749-11752. 10.1039/C8CC05597A.
[14] T. Weinrich, E.A. Jaumann, U.M. Scheffer, T.F. Prisner, M.W. Göbel, Phosphoramidite building blocks with protected nitroxides for the synthesis of spin-labeled DNA and RNA, Beilstein J Org Chem 14 (2018) 1563-1569. 10.3762/bjoc.14.133.
[15] J.M. Esquiaqui, E.M. Sherman, J.D. Ye, G.E. Fanucci, Conformational Flexibility and Dynamics of the Internal Loop and Helical Regions of the Kink-Turn Motif in the Glycine Riboswitch by Site-Directed Spin-Labeling, Biochemistry 55 (2016) 4295-4305. 10.1021/acs.biochem.6b00287.
[16] E.B. Butler, Y. Xiong, J.M. Wang, S.A. Strobel, Structural Basis of Cooperative Ligand Binding by the Glycine Riboswitch, Chemistry & Biology 18 (2011) 293-298. 10.1016/j.chembiol.2011.01.013.
[17] P.Z. Qin, I.S. Haworth, Q. Cai, A.K. Kusnetzow, G.P.G. Grant, E.A. Price, G.Z. Sowa, A. Popova, B. Herreros, H. He, Measuring nanometer distances in nucleic acids using a sequence-independent nitroxide probe, Nature Protocols 2 (2007) 2354-2365. 10.1038/nprot.2007.308.
[18] L.L. Huang, A. Serganov, D.J. Patel, Structural Insights into Ligand Recognition by a Sensing Domain of the Cooperative Glycine Riboswitch, Molecular Cell 40 (2010) 774-786. 10.1016/j.molcel.2010.11.026.
[19] M.Y. Kwon, S.A. Strobel, Chemical basis of glycine riboswitch cooperativity, Rna-a Publication of the Rna Society 14 (2008) 25-34. 10.1261/rna.771608.
[20] M.J. Moore, C.C. Query, Joining of RNAs by splinted ligation, Rna-Ligand Interactions Pt a: Structural Biology Methods 317 (2000) 109-123.
[21] K.J. Ellis, J.F. Morrison, Buffers of constant ionic-strength for studying pH-dependent processes, Methods in Enzymology 87 (1982) 405-426.
[22] R. E.E., B. R.R., In-Line Probing Analysis of Riboswitches, Humana Press, Methods in Molecular Biology, 2008.
[23] X.J. Zhang, P. Cekan, S.T. Sigurdsson, P.Z. Qin, STUDYING RNA USING SITE-DIRECTED SPIN-LABELING AND CONTINUOUS-WAVE ELECTRON PARAMAGNETIC RESONANCE SPECTROSCOPY, Methods in Enzymology, Vol 469: Biophysical, Chemical, and Functional Probes of Rna Structure, Interactions and Folding, Pt B 469 (2009) 303-328. 10.1016/s0076-6879(09)69015-7.
[24] T.M. Casey, Z.L. Liu, J.M. Esquiaqui, N.L. Pirman, E. Milshteyn, G.E. Fanucci, Continuous wave W- and D-Band EPR spectroscopy offer "sweet-spots" for characterizing conformational

changes and dynamics in intrinsically disordered proteins, Biochemical and Biophysical Research Communications 450 (2014) 723-728. 10.1016/j.bbrc.2014.06.045.
[25] J.M. Esquiaqui, E.M. Sherman, J.D. Ye, G.E. Fanucci, Site-directed spin-labeling strategies and electron paramagnetic resonance spectroscopy for large riboswitches, Methods Enzymol 549 (2014) 287-311. 10.1016/B978-0-12-801122-5.00013-1.
[26] D. Lambert, D.E. Draper, Effects of osmolytes on RNA secondary and tertiary structure stabilities and RNA-Mg2+ interactions, Journal of Molecular Biology 370 (2007) 993-1005. 10.1016/j.jmb.2007.03.080.
[27] K.M. Ruff, A. Muhammad, P.J. McCown, R.R. Breaker, S.A. Strobel, Singlet glycine riboswitches bind ligand as well as tandem riboswitches, Rna 22 (2016) 1728-1738. 10.1261/rna.057935.116.
[28] T. Hetzke, M. Vogel, D.B. Gophane, J.E. Weigand, B. Suess, S.T. Sigurdsson, T.F. Prisner, Influence of Mg2+ on the conformational flexibility of a tetracycline aptamer, RNA 25 (2019) 158-167. 10.1261/rna.068684.118.
[29] M. Mandal, M. Lee, J.E. Barrick, Z. Weinberg, G.M. Emilsson, W.L. Ruzzo, R.R. Breaker, A glycine-dependent riboswitch that uses cooperative binding to control gene expression, Science 306 (2004) 275-279. 10.1126/science.1100829.